PHYSICAL REVIEW E **74**, 061704 (2006)

Deuterium nuclear-magnetic-resonance study of a chiral smectic-C^* phase

J. Zhang,[1] A. Ferraz,[2,3] A. C. Ribeiro,[2,3] P. J. Sebastião,[2,3] and Ronald Y. Dong[1,4]
[1]*Department of Physics and Astronomy, University of Manitoba, Winnipeg, Manitoba, Canada R3T 2N2*
[2]*Centro de Física da Matéria Condensada, Avenida Prof. Gama Pinto 2, 1649-003 Lisbon, Codex, Portugal*
[3]*Departamento de Física, Instituto Superior Técnico, Avenida Rovisco Pais, 1049-001 Lisboa, Portugal*
[4]*Department of Physics and Astronomy, Brandon University, Brandon, Manitoba, Canada R7A 6A9*

(Received 3 November 2006; published 21 December 2006)

This study reports deuterium nuclear-magnetic-resonance (NMR) spectra collected at 61.4 MHz in the chiral smectic-C phase of liquid crystal 4′(octyloxy)-d_{17} biphenyl-4-*y*l2-chloro-3-methylpentanoate (BP8Cl). By using a goniometer probe, the oriented sample was rotated to collect spectra at different rotation (θ) angles. These spectra were simulated to gain information on solitonlike distortions in the helical superstructure. The Landau theory was adopted to study the distortion of the helix by the NMR magnetic field. Deuterium two-dimensional exchange experiments were also used on the aligned sample at $\theta=15°$ to obtain dynamic parameters through the spectral simulation. The interlayer diffusion constants in the SmC^* phase were estimated from a proton T_1 dispersion study. The pitch length of BP8Cl is estimated to be circa 2–3 microns at one temperature.

DOI: 10.1103/PhysRevE.74.061704 PACS number(s): 61.30.−v

I. INTRODUCTION

Since the discovery of synclinic ordering in ferroelectric chiral smectic-C (SmC^*) phase of chiral liquid crystals (LC) over three decades ago [1], significant experimental and theoretical efforts have been directed to study the structure and dynamics of chiral synclinic and anticlinic phases [2–7]. While rotational diffusion of molecules has been studied in chiral phases by measuring deuteron spin relaxation times [2,8], translational diffusion of molecules in these phases is harder to observe because of the very low self-diffusion constant, especially in anticlinic phases [7,9]. Spatial modulations of the local electric field gradient (EFG) of deuteron(s) by molecular self-diffusions along the helical axis is not effective in the SmC^* phase to affect the one-dimensional deuterium line shapes in angular-dependent nuclear-magnetic-resonance (NMR) studies. Recently a two-dimensional (2D) deuterium exchange experiment [10] has been applied to study jump diffusive motions in the SmC^* phase of an aligned chiral LC (10B1M7), and to directly detect the molecular self-diffusion in this phase [11]. Unfortunately, the self-diffusion constant cannot be uniquely obtained without a prior knowledge of the helical pitch length. Hence, the mentioned work has to assume a particular value for the pitch length. In the present study, we have applied the same technique to study self-diffusions in the SmC^* phase of 4′-(octyloxy)-$d17$ biphenyl-4-*y*l2-chloro-3-methylpentanoate (BP8Cl). To alleviate the above difficulty, we also employ the proton spin relaxation over a wide range of Larmor frequency in the same compound to shed light on the modulation of intermolecular interactions due to molecular self-diffusions. In this way, a consistent picture on the interlayer diffusion of molecules along the pitch axis is sought.

The effect of magnetic field on the SmC^* phase has been extensively studied [12,13]. Solitonlike distortions of the helical structure have been observed by various experimental techniques when the magnetic field is applied normal to the helical axis. If the magnetic field strength is high enough (either parallel or perpendicular to the pitch axis), the distorted helical structure will be unwound into a homogeneously ordered smectic C (uSmC^*) phase. A deuterium angular-dependent study has recently been reported on the investigation of solitonlike deformations in a SmC^* phase of another chiral LC (S)-[4-(2-methylbutyl)phenyl]-4′-octylbiphenyl carboxylate (8BEF5) [14]. The critical field for unwinding the helical structure has also been determined far away from the triple (Lifshitz) point [4] in the (H,T) phase diagram. In 8BEF5, the angular variation in the sample rotation experiments at each temperature is, however, limited to small angles (<25°). The general Landau theory [12,15] can only be tested within this small range of angle. In the present study, BP8Cl has been chosen, even though its SmC^* phase at 9.4 T has a rather narrow temperature range, to critically test the Landau theory over a wide range of sample rotation angles in the NMR magnetic field. The paper is organized as follows. Section II contains the experimental method. Section III gives the relevant theory to describe simulations of experimental results, and to extract interlayer jump diffusion constants in the SmC^* phase. Section IV gives the results and discussion. The last section gives a brief conclusion.

II. EXPERIMENTAL METHOD

The chiral liquid crystal BP8Cl shows various mesophases (smectic A and chiral smectic-C) at different ranges of temperature. Its molecular structure is sketched in Fig. 1(a), together with the deuterium labels. The transition temperatures of BP8Cl, determined by our ^2H NMR study at a magnetic field of 9.4 T, are as follows

$$\text{Iso} \overset{337K}{\leftrightarrow} \text{Sm}A \overset{325K}{\leftrightarrow} u\text{Sm}C^* \overset{316K}{\leftrightarrow} \text{Sm}C^* \overset{303.3K}{\leftrightarrow} \text{Crystal},$$

where a uSmC^* phase is observed due to the applied magnetic field. The sample was aligned by slowly cooling to the

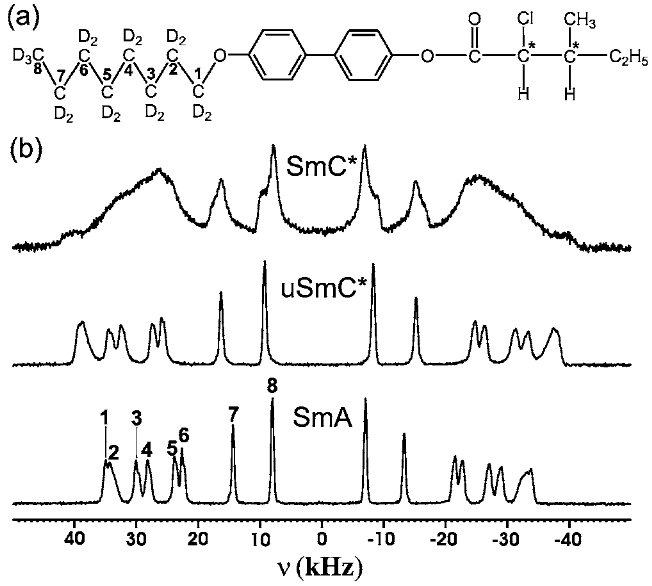

FIG. 1. (a) Molecular structure of a partially deuterated BP8Cl showing deuteron site labels. (b) Typical ^2H NMR spectra collected in different LC phases. Peak assignments are labeled in the lower spectrum.

desired temperature in the SmC^* phase after heating to the clearing temperature. The deuterium NMR studies were carried out using a Bruker goniometer probe equipped with a high precision pneumatic motor (better than 0.1° resolution) and a Bruker Avance 400 solid state system. The temperature of the sample was regulated with an airflow and the temperature gradient across the sample was estimated to be better than 0.5 degree. Enough waiting time between each temperature change was taken to assure temperature stabilization and equilibration. A $90_x{}^\circ-\tau-90_y{}^\circ-\tau$ solid echo pulse sequence was used to generate ^2H spectra at different sample rotation angles θ. The 90° pulse width was 2.6 μs. Number of scans needed to observe a good free induction decay (FID) or its Fourier transform was 32 and the recycle time between scans was 1 s. Typical deuterium one-dimensional (1D) spectra without rotating the sample in different phases are plotted in Fig. 1(b). To obtain spectra at nonzero θ, they were collected immediately (<1 s) after rotating the aligned sample a high θ angle in the magnetic field in order to avoid any time dependent sample degradation from the probable orientational flows. In order to collect another spectrum at this or other rotation angle, the sample was realigned by first heating into the isotropic phase. In the present study, we focus on the methyl deuterons at the last carbon site C_8 whose deuteron spin-lattice relaxation times are the largest.

2D deuterium "cosine" and "sine" exchange spectra were collected using a five-pulse sequence $90°-\tau-90°-\tau-t_1-54.7°-t_{mix}-54.7°-\tau-90°-\tau$ [16] with different phases of the two 54.7° pulses, where $\tau=30$ μs was the delay for the two refocusing 90° pulses. To get a good FID signal in the SmC^* phase, we needed to average FID after the last 90° pulse 64 scans for each t_1 value. Before obtaining a 2D exchange spectrum, the aligned sample was first rotated in the goniometer probe by 15 degrees. The field-induced sample realignment during the 2D exchange experiment was found to be negligible by reproducing the 1D deuterium spectrum immediately after collecting each 2D exchange spectrum. The exchange mixing time t_{mix} was chosen according to the molecular jump constant, and t_1 gave the time increment in the F1 dimension. The recycle time between scans was 1 s. With a typical number of 80 t_1 increments, about 1.5 h was required to obtain a 2D exchange spectrum. The pure absorption mode spectrum was obtained by adding the experimental cosine and sine spectra.

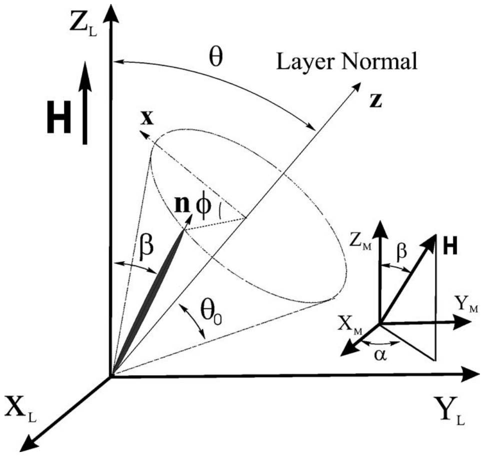

FIG. 2. The geometry of a sample rotation experiment. **n** is the molecular director. (X_L, Y_L, Z_L) is the laboratory frame, (X_M, Y_M, Z_M) is the molecular frame, whereas the (x,y,z) frame is fixed to the LC smectic layers.

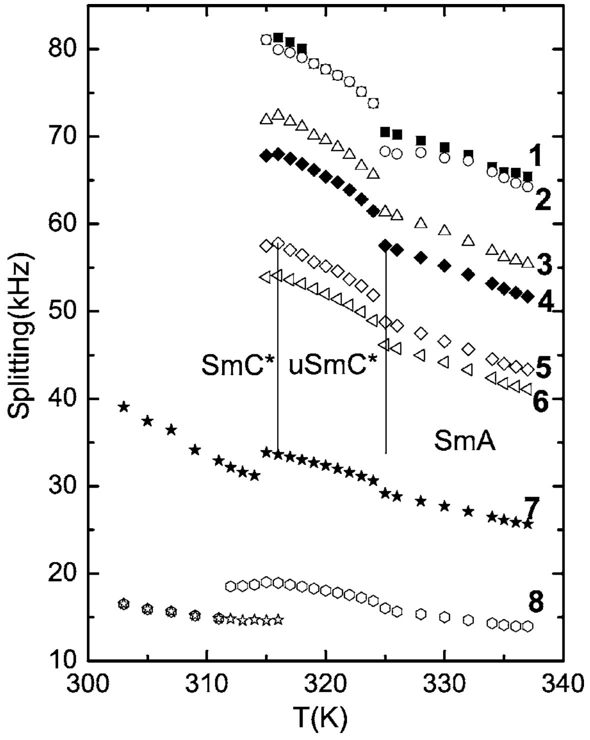

FIG. 3. Plot of quadrupolar splittings of BP8Cl versus the temperature. Deuteron lines are labeled by their carbon numbers.

III. THEORETICAL BACKGROUND

When the ferroelectric LC ($\Delta\chi > 0$) sample is initially magneto-aligned by the NMR magnetic field H, the pitch axis is oriented along the external magnetic field in the SmC^* phase. The ^2H spin(s) produces a spectrum of two lines with spectral frequencies given by [17]

$$\nu^{\pm} = \pm \frac{3}{4}\bar{\nu}_Q\left(\frac{3}{2}\cos^2\beta - \frac{1}{2} + \frac{\bar{\eta}}{2}\sin^2\beta\cos 2\alpha\right) \qquad (1)$$

where $\bar{\nu}_Q = eQ\bar{V}_{zz}/h$ is a time-averaged nuclear quadrupolar coupling constant along the long molecule (Z_M) axis, $\bar{\eta}$ is a time-averaged asymmetry parameter, and β, α are the polar angles of the applied H field in the molecule-fixed frame (see Fig. 2). At a sufficiently high magnetic field, the helix can show solitonlike distortions. At temperatures far away from the Lifshitz point, the distortion can be treated by a general Landau theory under the constant amplitude approximation [4]. The helix is usually more easily distorted by applying the magnetic field normal to the pitch axis. As the NMR field is fixed, the aligned sample is rotated by an angle θ in a goniometer probe in order to have a nonzero field component in the direction perpendicular to the pitch axis. When the pitch axis is set at a nonzero θ angle with respect to the NMR field, β can be obtained from the geometry to give

$$\cos\beta = \sin\theta\sin\theta_0\cos\phi + \cos\theta\cos\theta_0, \qquad (2)$$

where θ_0 is the molecular tilt angle and ϕ is the molecular azimuthal angle measured with respect to the plane formed by the layer normal and the H field (i.e., with respect to the x axis in Fig. 2). As seen in Fig. 2, the observed spectrum from the rotated sample is the sum of frequencies from molecules uniformly distributed on the surface of a cone for an undistorted helical structure. Furthermore, it contains two or three singularities (s_1, s_2, s_3), and by fitting the angular-dependent positions of the singularities $\bar{\eta}$, $\bar{\nu}_Q$, and θ_0 can be determined from [17],

$$s_1^{\pm} = \pm\frac{3}{4}\bar{\nu}_Q\left[1 - \frac{1}{2}(3-\bar{\eta})\sin^2(\theta - \theta_0)\right]$$

$$s_2^{\pm} = \pm\frac{3}{4}\bar{\nu}_Q\left[1 - \frac{1}{2}(3-\bar{\eta})\sin^2(\theta + \theta_0)\right]$$

and when $\frac{\pi}{2} \geqslant \theta \geqslant \tan^{-1}[(3-\bar{\eta})\sin 2\theta_0/((3-\bar{\eta})2\sin^2\theta_0 + 4\bar{\eta})]$

$$s_3^{\pm} = \pm\frac{3}{4}\bar{\nu}_Q\left[\frac{(3+\bar{\eta})\bar{\eta}\cos^2\theta}{(3-\bar{\eta})\sin^2\theta_0 + 2\bar{\eta}} - \frac{1}{2}(1+\bar{\eta})\right]. \qquad (3)$$

Note that s_1 and s_2 correspond to the frequencies at $\phi = 0°$ and 180°, respectively.

If a uniform ϕ distribution in the helix is distorted by the NMR magnetic field to give a new ϕ distribution [$d\phi/dz \propto \Omega(\phi)$] [4,14], the critical field (H_c^0) for unwinding the helical structure in the SmC^* phase can be obtained by fitting the observed (distorted) spectra to the ones calculated from the Fourier transform of FID given by the following integral [4,14,18]:

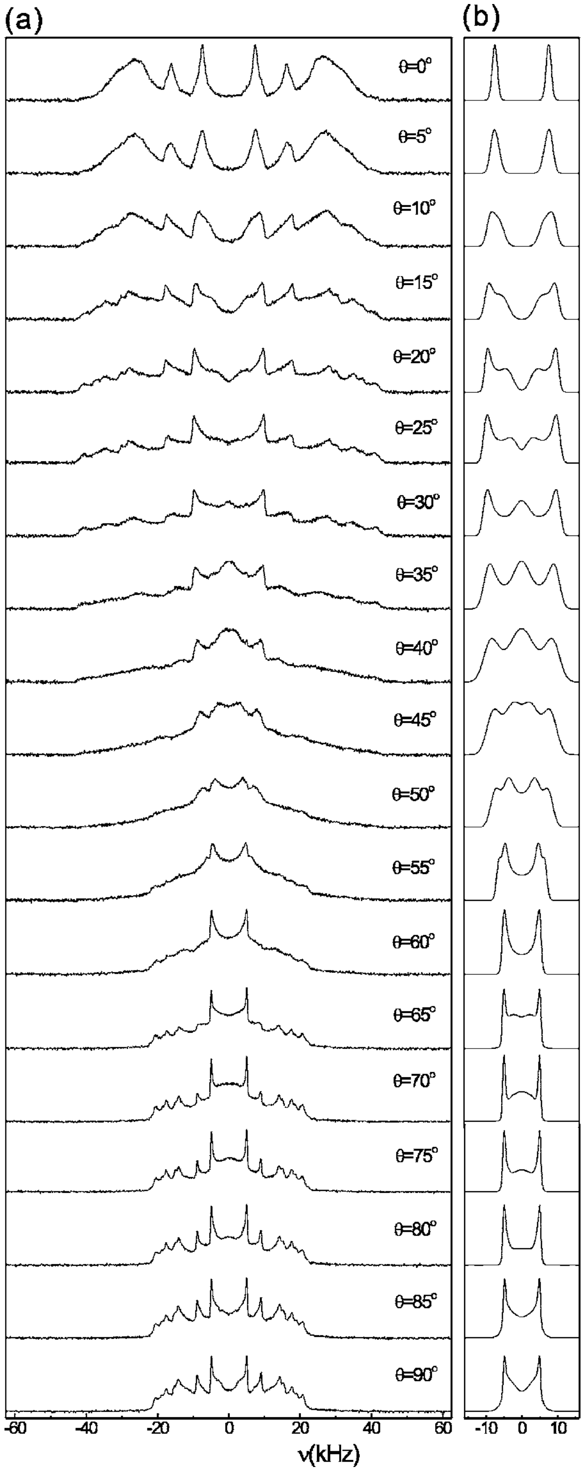

FIG. 4. (a) Experimental and (b) Simulated angular dependent ^2H NMR line shapes in the SmC^* phase of BP8Cl at 311.5 K.

$$I(\theta_0,t) = I(\theta_0,0)\int_0^{2\pi}\frac{1}{\Omega(\phi)}\int\Gamma(\theta_0' - \theta_0) \times\cos(2\pi\nu(\phi,\theta,\theta_0')t)\,d\theta_0' e^{-\sigma^2t^2/2}d\phi, \qquad (4)$$

where $\nu(\phi,\theta,\theta_0)$ is obtained from Eqs. (1) and (2), and a

Gaussian distribution is assumed [19] here for the distribution of the local director, i.e.,

$$\Gamma(\theta_0' - \theta_0) = \frac{1}{\omega\sqrt{2\pi}} e^{-(\theta_0' - \theta_0)^2/2\omega^2} \tag{5}$$

with 1.18ω being the half width at half maximum of the distribution, $e^{-\sigma^2 t^2/2}$ to account for the spectral line broadening by a fitting parameter σ. Now $\Omega(\phi) = \sqrt{1+1/(4A)-\kappa^2(\cos 2\phi/(4A)+\cos\phi)}$, where $A = \cot\theta \cot\theta_0$, is found from minimizing the Landau free energy density and κ is an integration constant in finding the ϕ distribution. Now $\kappa(H/H_c^0, \theta)$ is treated as a fitting parameter, and is related to the critical field H_c^0 and the rotation angle by [14],

$$\frac{e(\kappa)}{\kappa} = \sqrt{\frac{\tan\theta_0}{\sin 2\theta}\frac{4H_C^0}{H}}. \tag{6}$$

In the above equation $e(\kappa)=\int_0^{2\pi}\Omega(\phi)d\phi$, and H_C^0 is the critical magnetic field to unwind the helix when it is applied normal to the pitch axis. When $\kappa=0$, $\Omega(\phi)$ is constant, while uSmC^* phase is obtained when $\kappa=1$. In the SmC^* phase, the order parameter is high, thereby leading to a small ω value. Under this condition, $I(\theta_0,t)$ can be rewritten [14]

$$I(\theta_0,t) = I(\theta_0,0)\int_0^{2\pi}\frac{1}{\Omega(\phi)}\cos(2\pi\nu(\phi,\theta,\theta_0)t) \times e^{-\sigma^2 t^2/2-(2\pi\omega[\partial\nu/\partial\theta_0])^2 t^2} d\phi. \tag{7}$$

The observed line shape is simulated by Fourier transforming Eq. (7) numerically. By comparing the simulated 1D spectra with the corresponding experimental spectra, the critical field for unwinding the helix at a certain temperature can be obtained using Eq. (6).

When molecules diffuse along the pitch axis, the molecule tilt direction (θ_0,ϕ) will change by following the tilt direction in each smectic layer. In the SmC^* phase, the tilt direction changes the azimuthal angle by a tiny amount between the neighboring layers. As a result, modulation of the NMR frequency by molecular self-diffusions is small over a short distant scale, and is hard to be detected in a 1D spectrum [7]. A two-dimensional exchange experiment can give a model-independent reorientational process of molecules for slow dynamic situations [10]. Considering that a pitch length usually includes hundreds of smectic layers, we assume that the azimuthal angle (ϕ) of the molecular tilt is a linear function of diffusion length l along the pitch axis z, *viz.* the tilt direction will change by $\delta\phi=2\pi l/P_t$, where P_t is the pitch length. The assumption is considered a good approximation even in the case of small solitonlike distortions. This is rationalized by the fact that the solitonlike region is vanishingly small in comparison to the pitch length. The interlayer self-diffusion is a one-dimensional diffusion problem, and the probability $P(\phi_0,\phi,t)$ of finding a molecule at position ϕ and at time t given a position ϕ_0 at $t=0$ is [20]

$$P(\phi_0,\phi,t) = \frac{P_t}{\sqrt{16\pi D t}} e^{-(\phi-\phi_0)^2/16\pi^2 \varsigma t}, \tag{8}$$

where D is a translational self-diffusion constant, and $\varsigma = D/P_t^2$ is treated as a fitting parameter. The 2D exchange spectrum $S(f_1,f_2;\phi_0)$ can be calculated from summing the cosine (cc) and sine (ss) spectra, which are the Fourier transform of the FIDs given by the following integrals [11]

$$I_{cc}(t_1,t_2;\phi_0,t_{mix}) = \int\int\frac{P(\phi_0,\phi,t_{mix})}{\Omega(\phi)\Omega(\phi_0)}\cos[2\pi\nu(\phi)t_2]\cos[2\pi\nu(\phi_0)t_1]R'(\phi,\phi_0,t_1,t_2)d\phi d\phi_0,$$

$$I_{ss}(t_1,t_2;\phi_0,t_{mix}) = \int\int\frac{P(\phi_0,\phi,t_{mix})}{\Omega(\phi)\Omega(\phi_0)}\sin[2\pi\nu(\phi)t_2]\sin[2\pi\nu(\phi_0)t_1]R'(\phi,\phi_0,t_1,t_2)d\phi d\phi_0, \tag{9}$$

where $R'(\phi,\phi_0,t_1,t_2)=\exp\left[-\sigma^2(t_1^2+t_2^2)/2-\left(2\pi\omega\frac{\partial\nu}{\partial\theta_0}\right)^2_{\phi_0} t_1^2 - \left(2\pi\omega\frac{\partial\nu}{\partial\theta_0}\right)^2_{\phi} t_2^2\right]$ is to account for the spectral line broadening, and $\nu(\phi)$ is again given by Eqs. (1) and (2). It is important to realize that the slice of this 2D spectrum with $f_1=\nu(\phi_0)$ is given by Fourier transforming the following FID with respect to t_2,

$$I(t_2) = \int\frac{P(\phi_0,\phi,t_{mix})}{\Omega(\phi)}\{\cos[2\pi\nu(\phi)t_2] + \sin[2\pi\nu(\phi)t_2]\} e^{-\sigma^2 t_2^2/2-(2\pi\omega[\partial\nu/\partial\theta_0])^2_{\phi} t_2^2} d\phi. \tag{10}$$

Fixing ω and κ values to those obtained in the 1D simulation, one can in principle get D by simulating the 2D spectrum using Eq. (9).

IV. RESULTS AND DISCUSSION

The observed deuterium splittings are plotted versus the temperature in Fig. 3. As seen in this diagram, only the quadrupolar splitting of C_7 and C_8 can be discerned in the SmC^* phase due to the severe line broadening. Furthermore, the transition between the uSmC^* and SmC^* phase in BP8Cl involves a biphasic region (about 4 degrees) clearly seen from the C_8 signals. Figure 4(a) shows a typical set of angle-dependent spectral patterns observed at 311.5 K. Our experi-

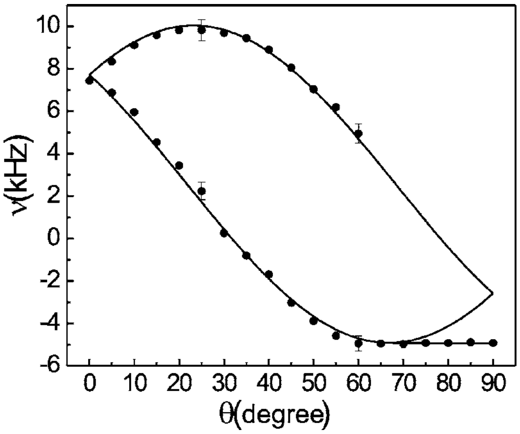

FIG. 5. Plot of the angular-dependent singularities ($2|s_i|$) in BP8Cl at 311.5 K (●). The solid lines are fitted curves.

ments show that at this temperature there is no observable field-induced sample reorientation and layer destruction. This was checked experimentally by reproducing the measurement after waiting for half an hour. It should be noted that the present sample behaves quite differently from the smectogen 8BEF5 [14], *viz.* the C_α deuteron(s) of 8BEF5 shows edge singularities only at small rotation angles ($\theta < 25°$). The angular-dependent characteristic singularities at this temperature are shown in Fig. 5. The solid lines in this figure are fitted curves using Eq. (3) to give $\bar{\nu}_Q = 10.0$ kHz, $\theta_0 = 23.3°$, and $\bar{\eta} = 0$ at 311.5 K. The last quantity signifies that the present SmC^* phase is not biaxial. Note that θ can now extend to 90°. Hence, BP8Cl could provide a better test of the Landau theory. When fitting the angular-dependent ^2H NMR line shapes, the tilt angle and time-averaged coupling constant were set at $\theta_0 = 23.3 \pm 0.2°$ and $\bar{\nu}_Q = 10.0 \pm 0.5$ kHz. For a known rotation angle θ, the integration constant κ was varied to give the "best" simulated line shapes for C_8 deuterons shown in Fig. 4(b). The line broadening parameters σ and ω were also fitted to reflect the observed linewidths. The fitting parameters for different angles are summarized in Table I. We note that κ was nonzero when the sample was rotated by an angle away from the external magnetic field, which meant that the helical structure had some solitonlike behaviors. Since the spectral linewidth seemed to change with θ, the line broadening parameter σ was varied between 1.6−9 at different rotation angles. This variation only changed the linewidth without affecting the spectral features. Thus, κ was uniquely obtained and independent of other parameters.

TABLE I. Fitting parameters in the spectral simulation for different θ at 311.5 K.

θ(deg)	$\kappa(\pm 0.02)$	σ(kHz)(± 0.3)	ω(deg)(± 0.2)
0	0	4.5	0
5	0.35	3.5	0.45
10	0.45	5	0.45
15	0.63	5	0.52
20	0.70	4	0.55
25	0.75	5	0.55
30	0.80	5.5	0.35
35	0.82	7	0.7
40	0.85	9	0.75
45	0.86	6	0.75
50	0.84	6.5	0.3
55	0.84	3.5	0.1
60	0.85	2.5	0.2
65	0.84	2	0.65
70	0.80	1.8	1
75	0.70	1.7	1
80	0.70	1.7	0.8
85	0.98	1.6	1.3
90	0.98	1.6	1.3

We had also simulated the line shapes at 308.5 K to give $\bar{\nu}_Q = 10.4 \pm 0.5$ kHz and $\theta_0 = 25.0 \pm 0.2°$. Figure 6 shows plots of $\kappa/e(\kappa)$ versus $\sqrt{(\sin 2\theta)}$ for θ between 0° and 90° at these temperatures, and according to Eq. (6), the slope determines the critical field at a particular temperature. From Fig. 6, H_c^0 is seen to decrease slightly with increasing temperature in qualitative agreement with the theoretical prediction [13]. The magnitude of H_c^0 for BP8Cl is on the order of 29.9 T at low temperature which is about a factor of 3 higher than the NMR field used in this study. At higher temperatures, the critical fields must be lower ($\sim$9 T) in order to produce the uSmC^* phase. It would appear that the sample viscosity and flow behaviors must be rather sensitive to temperature. Unfortunately, at the present magnetic field, the SmC^* phase only exists in a narrow temperature range, thereby excluding a detailed study of $H_c(T)$ in BP8Cl. Several 2D exchange spectra were collected at 311.5 K in the SmC^* phase with different mixing times. It is important to have the aligned sample rotated away from the magnetic field (here $\theta = 15°$) in order to detect interlayer molecular self-diffusions. Our ex-

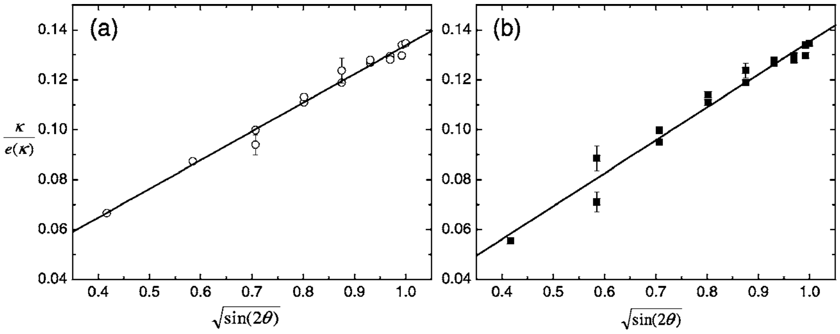

FIG. 6. Plot of $\kappa/e(\kappa)$ versus $\sqrt{(\sin 2\theta)}$ for (a) 308.5 K (circle) and (b) 311.5 K (square). The solid lines are fitted lines according to Eq. (6). The H_c^0 is found to be 29.9 ± 2 T and 27.0 ± 5 T at 308.5 K and 311.5 K, respectively.

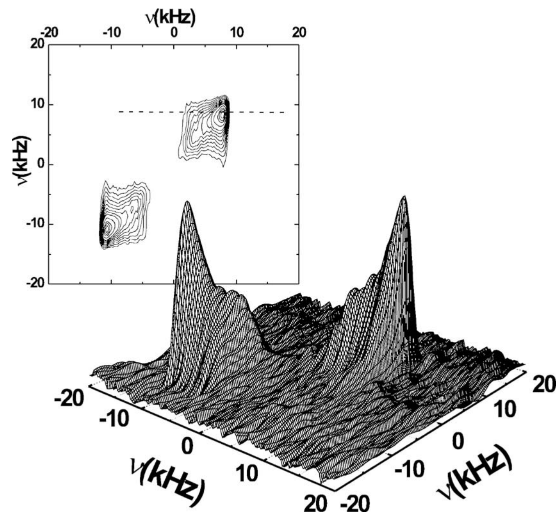

FIG. 7. Plots of 2D ^2H exchange spectrum in the SmC^* phase at 311.5 K, $\theta=15°$, and $t_{mix}=300$ ms. The spectrum was symmetrized with respect to the diagonal axis. Only the signal of the methyl deuterons (C_8) is emphasized in the surface plot and the vertical axis for intensity has been omitted for clarity. Dashed line in the contour plot is the slice that is shown in Fig. 9.

periment showed that it was hard to observe the cross peaks for $t_{mix}<100$ ms, and there was no significant change in the 2D exchange spectra when $t_{mix}>700$ ms. Because of the serious overlaps among the ^2H peaks, only the C_8 signal is emphasized in the 2D spectrum shown here. Figure 7 shows the 2D spectrum collected with $t_{mix}=300$ ms, while Fig. 8 shows the contour plots of $t_{mix}=150$ and 500 ms. Note that all other experimental parameters are identical for these 2D exchange spectra. The 2D exchange spectrum was hard to be simulated, especially because of the spectral overlap from the neighboring deuterons; instead 1D spectrum obtained from the slice $f_1=s_1$ [or $f_1=\nu(0)$] in a 2D spectrum (see dashed line in Figs. 7 and 8) was more easily fitted. These 1D slices for several mixing times at 311.5 K are shown in Fig. 9. Four parameters θ_0, κ, σ, ω were fixed to values obtained in the 1D spectrum simulation [Fig. 4(b)], and the ς value was varied to get the best dashed spectra shown in Fig. 9. A ς value of 0.13 ± 0.1 s^{-1} was obtained from the fitting of all slices at different mixing times [20]. The simulated 2D exchange spectrum was then reconstructed (Fig. 10) using the above derived fitting parameters and its agreement with Fig. 7 is good. The self-diffusion constant can now be derived from ς and the pitch length, based on $D=\varsigma P_t^2$. However, the pitch length P_t is unknown for BP8Cl. Fortunately proton NMR T_1 dispersion study has been performed at $\theta=0°$ in BP8Cl (Fig. 11 and the detailed analyses will be published elsewhere [21]. Suffice to say that the proton T_1 dispersion over a wide range of Larmor frequency (4 kHz to 300 MHz) can be attributed to three different relaxation contributions: collective motions (C), individual molecular rotations (R), and molecular translational self-diffusions (SD) [22]. Correlation times associated with the local reorientations and with the translational SD were esti-

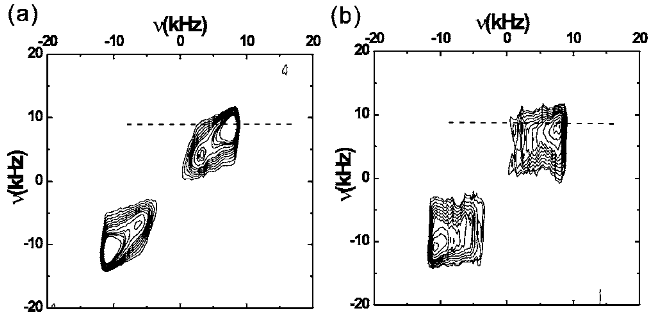

FIG. 8. Contour plots of 2D ^2H exchange spectra in the SmC^* phase at 311.5 K and $\theta=15°$. (a) $t_{mix}=150$ ms, (b) $t_{mix}=500$ ms. Dashed line in the contour plot gives the 1D spectrum at a particular mixing time shown in Fig. 9.

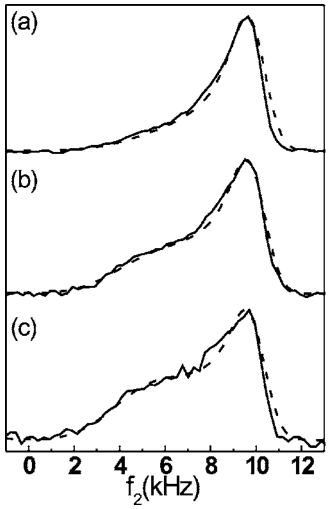

FIG. 9. One-dimensional slices (solid lines) taken from the 2D exchange spectra shown in Figs. 7 and 8 for (a) $t_{mix}=150$ ms, (b) $t_{mix}=300$ ms, (c) $t_{mix}=500$ ms. The simulated spectra (dashed lines) are obtained with $\varsigma=0.13$ s^{-1}, and κ was fixed at 0.63.

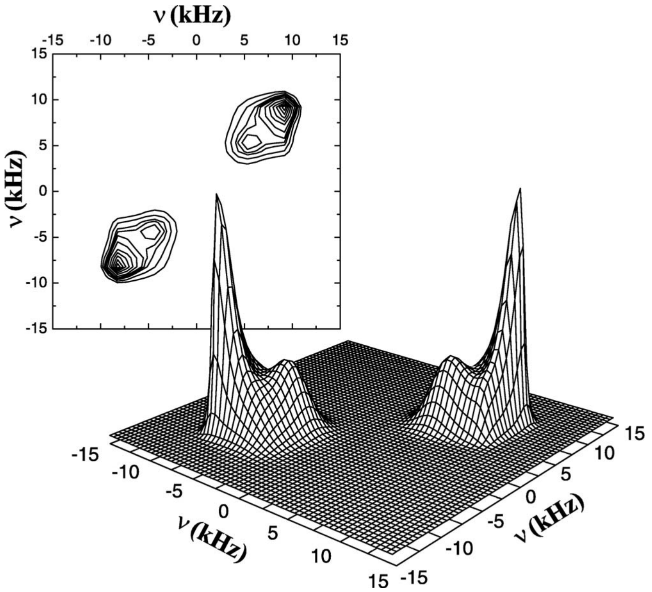

FIG. 10. Simulated 2D ^2H exchange spectrum and contour plot at $t_{mix}=150$ ms. The vertical axis in the surface plot is omitted.

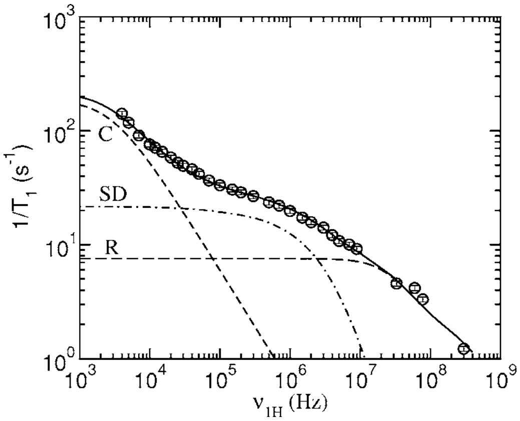

FIG. 11. Proton $1/T_1$ dispersion in the SmC^* phase at 322 K and best fits to the molecular mechanisms: collective motion (C), translational self-diffusion (SD), and local rotations/reorientations (R).

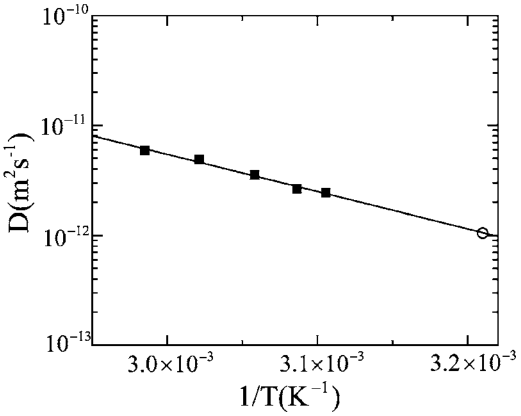

FIG. 12. Translational self-diffusion constants obtained from the fits of T_1 (squares) dispersion. Arrhenius fit to the self-diffusion values (solid line) allows to estimate the D value at 311.5 K (circle).

mated from a model fit analysis of the proton T_1 dispersion curve at each temperature. As seen in Fig. 11, it is observed that rotations/reorientations are clearly decoupled from the SD contribution in the T_1 dispersion graph. The diffusion constant D has, therefore, been obtained at several temperatures in the SmA and SmC^* phase (Fig. 12). Assuming the usual Arrhenius temperature dependence for the translational self-diffusion, a value of $D=1.1\times10^{-12}\ \mathrm{m}^2/\mathrm{s}$ has been estimated for $T=311.5$ K.

This D value and $\varsigma=0.13\ s^{-1}$ lead to a pitch length of $2.9\pm0.7\ \mu$m, which seems quite reasonable in comparison with typical pitch lengths (few microns) in SmC^* phases. It has also been reported [23] in the literature that in one instance of SmC^* phase the pitch length can range up to about 9.5 μm. Apart from the uncertainty in the estimated D value, the observed P_t value could be larger due to the fact that partial unwinding (or distortion) could exist even at $\theta=15°$ ($\kappa\neq0$). It should be noted that the present technique to obtain the self-diffusion constant cannot be achieved at $\theta=0°$. The reconstructed 2D exchange spectra for $t_{mix}=150$ ms (Fig. 10), 300 ms, and 500 ms are found in good agreement with the observed 2D spectra.

V. CONCLUSION

In this work, both the angular-dependent spectral technique and 2D exchange experiments are used to study helical distortions over a wide angle range (up to 90°) and the dynamics in the chiral SmC^* phase. In the SmC^* phase, the tilt direction changes azimuthally from one layer to another layer to form a helix. By rotating the sample in a goniometer probe, the ^2H NMR spectra reflect the change in the orientational distribution with respect to the H field and/or partial "unwinding" of the helix. Spectral line shape simulation was used to give the tilt angles at different temperatures. Moreover, Landau theory is successfully used in the simulation to get the critical field for BP8Cl. The 2D exchange experiments are useful to reveal the self-diffusion of molecules in the SmC^* phase. By fitting 1D slices and 2D experimental spectra, the diffusion constant can be estimated provided that the pitch length is known by another means. In particular, proton T_1 dispersion measurement was used to get an estimated D value at 311.5 K. This puts an upper limit on the pitch length of 2.9 μm at one temperature.

ACKNOWLEDGMENTS

The Natural Sciences and Engineering Council of Canada, Canada Foundation of Innovation and Brandon University are thanked for their financial support. We thank H. T. Nguyen for providing the deuterated compound.

---

[1] R. B. Meyer, L. Liebert, L. Strzelecki, and P. Keller, J. Phys. (Paris) **36**, L69 (1975).

[2] R. Y. Dong, L. Chiezzi, and C. A. Veracini, Phys. Rev. E **65**, 041716 (2002).

[3] Y. Galerne and L. Liebert, Phys. Rev. Lett. **66**, 2891 (1991).

[4] B. Zalar, A. Gregorovic, M. Simsic, A. Zidansek, R. Blinc, S. Keast, and M. Neubert, Phys. Rev. Lett. **80**, 4458 (1998).

[5] P. V. Dolganov, B. M. Bolotin, and A. Fukuda, Phys. Rev. E **70**, 041708 (2004).

[6] P. Mach, R. Pindak, A.-M. Levelut, P. Barois, H. T. Nguyen, C. C. Huang, and L. Furenlid, Phys. Rev. Lett. **81**, 1015 (1998).

[7] B. Zalar, A. Gregorovic, and R. Blinc, Phys. Rev. E **62**, R37 (2000).

[8] D. Catalano, L. Chiezzi, V. Domenici, M. Geppi, C. Veracini, R. Dong, and K. Csorba, Macromol. Chem. Phys. **203**, 1594 (2002).

[9] M. Cifelli, V. Domenici, and C. A. Veracini, Mol. Cryst. Liq. Cryst. **429**, 167 (2005).

[10] K. Schmidt-Rohr and H. W. Spiess, *Multidimensional Solid-State NMR and Polymers* (Academic Press, New York, 1994).

[11] J. Xu and R. Y. Dong, J. Phys. Chem. B **110**, 1221 (2006).
[12] I. Musevic, B. Zeks, R. Blinc, T. Rasing, and P. Wyder, Phys. Rev. Lett. **48**, 192 (1982).
[13] B. Kutnjak-Urbanc and B. Zeks, Phys. Rev. E **48**, 455 (1993).
[14] cJ. Xu, C. A. Veracini, and R. Y. Dong, Chem. Phys. Lett. **416**, 47 (2005).
[15] L. D. Landau and E. M. Lifshitz, Am. J. Phys. **27**, 371 (1959).
[16] D. Schaefer, J. Leisen, and H. W. Spiess, J. Magn. Reson., Ser. A **115**, 60 (1995).
[17] B. G. Wu and J. W. Doane, J. Magn. Reson. (1969-1992) **75**, 39 (1987).
[18] J. Xu, C. A. Veracini, and R. Y. Dong, Phys. Rev. E **72**, 051703 (2005).
[19] A. Firouzi, D. J. Schaefer, S. H. Tolbert, G. D. Stucky, and B. F. Chmelka, J. Am. Chem. Soc. **119**, 9466 (1997).
[20] J. Crank, *Mathematics of Diffusion* (Oxford University Press, Oxford, 1975).
[21] A. Ferraz *et al.* (unpublished).
[22] A. Carvalho, P. J. Sebastião, A. Ribeiro, H. T. Nguyen, and M. Vilfan, J. Chem. Phys. **115**, 10484 (2001).
[23] B. I. Ostrovskii, A. Z. Rabinovich, A. S. Sonin, and B. A. Strukov, Sov. Phys. JETP **47**, 912 (1978).